Astron. Astrophys. 358, 1027–1034 (2000)

ASTRONOMY
AND
ASTROPHYSICS

# X-ray activity in T-Tauri stellar magnetospheres

**G.T. Birk, D. Schwab, H. Wiechen, and H. Lesch**

Institut für Astronomie und Astrophysik der Universität München, Scheinerstrasse 1, 81679 München, Germany

Received 18 January 2000 / Accepted 13 April 2000

**Abstract.** X-ray flares belong to magnetic activity phenomena that are characteristic for T-Tauri stars. The relatively strong magnetic fields of T-Tauri magnetospheres can be regarded as the primary energy source for the flares. The energy can be converted to particle acceleration and plasma heating by reconnection events in twisted flux tubes that connect the central object and the circumstellar disk. Considering the whole range of the dynamic plasma parameters involved, i.e. the partially ionized dusty plasma regime, the partially ionized dust-free one and eventually, the totally ionized one, it becomes obvious that the localized dissipation of free magnetic energy is efficient and fast enough to overcome the radiative cooling. Model results that take into account ionization as well as dust evaporation/sublimation and the temporal varying resistivity indicate that in course of the dynamics of the resistive tearing instability the plasma in magnetospheric flux tubes can be heated up to X-ray temperatures.

**Key words:** X-rays: stars – stars: flare – stars: magnetic fields

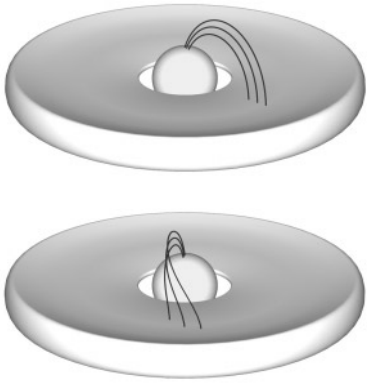

**Fig. 1.** Illustration of the magnetic coupling of the T-Tauri star with the circumstellar disk. The upper plot shows magnetic field lines without shear, the lower one the magnetic shear which is caused by the rotation. The magnetic shear is associated with current sheets that are unstable against tearing modes. The sheared magnetic flux tubes are the sites of X-ray emission.

## 1. Introduction

Variable thermal keV X-ray emission is identified as an ubiquitous phenomenon of classical and weak line T-Tauri stars (TTS) by the Einstein X-ray Observatory (Feigelson & DeCampli 1981) and more recently by the ROSAT and ASCA satellites (e.g. Carkner et al. 1996; Gullbring et al. 1997; for an overview see Feigelson & Montmerle 1999). This emission stems from a relatively high density plasma at a temperature of typically about $T_{\rm X} \sim 10^7$ K; even superhot flares with $T_{\rm X} \sim 10^8$ K have recently been detected (Tsuboi et al. 1998). X-ray flares in TTS with typical durations of $t_{\rm X} \sim 10^3 - 10^4$s are expected (e.g. Hayashi et al. 1996) to occur in magnetic flux tubes with spatial extents of $l_{\rm X} \sim 10^{10} - 10^{11}$ cm. Luminosities are found to be $L_{\rm X} \sim 10^{31}{\rm ergs}^{-1}$ or even higher (cf. Preibisch et al. 1993). Thus, X-ray flares in TTS are widely considered as upscaled versions of solar flares. As for the sun magnetic reconnection can be expected to play the key role for the observed variety of magnetic activity phenomena in TTS. Hayashi et al. (1996) proposed a model for the X-ray activity in classical TTS based on reconnection driven by the interaction of the stellar object and the circumstellar disk. Birk (1998) showed in a more quantitative analysis of tearing modes for the relevant partially ionized dusty plasma regime that the magnetic energy stored in magnetic flux tubes can efficiently and fast enough be converted to particle acceleration and thus, may be responsible for non-thermal radio emission. In both descriptions the continuous injection of magnetic helicity (cf. also Li 1996) in the closed flux tubes that connect the central object and the disk plays the dominant role for the energy support (see Fig. 1). These flux tubes are the sites of X-ray emission. Thus, one has to expect different sizes of emission regions depending on the extension of the respective reconnecting flux tube. The real magnetic configuration is even more complicated than the one illustrated in Fig. 1, since the Balbus Hawley instability and accretion flows will also distort the magnetic field heavily (see e.g. Miller & Stone 1997; Hirose et al. 1997 who modelled the meridional plane of the configuration shown in Fig. 1). However, for our purposes it is sufficient to realize that, in fact, the star-disk coupling is characterized by sheared magnetic fields. T-Tauri magnetospheres are constituted of sheared magnetic flux tubes associated with current sheets. These current sheets are unstable against tear-

*Send offprint requests to*: G.T. Birk

ing modes and thus, the magnetic energy can be converted to heat via reconnection. The situation is comparable to the rapid bursters in the context of neutron stars (cf. Kuijpers & Kuperus 1995) and to particle acceleration events in the magnetospheres of active galactic nuclei (Lesch & Birk 1997; Schopper et al. 1998). Neither Hayashi et al. (1996) nor Birk (1998) discussed in detail the heating process of the plasma caused by the fast dissipation of magnetic energy during the reconnection event. In fact, in order to corroborate the view that magnetic reconnection can be responsible for the thermal X-ray flares in TTS one has to show that the heating is both fast and efficient enough to fit the observational constraints and to overcome the cooling mechanisms. In doing this one has to consider in detail the changing physical parameters starting from a cold partially ionized dusty plasma. In the next section we estimate the heating rate on the grounds of a linear mode analysis of the tearing instability for different plasma parameter regimes that are expected to be involved in the entire flare process and compare this rate to the cooling rate given by the universal cooling function. We start from a rather cold partially ionized dusty plasma characteristic for the diskward parts of the considered magnetic flux tubes. Here, the reconnection process is probably initiated due to a finite collisional resistivity. We note that dust particles can also be injected in the flux tubes during accretion and thereby contribute to the violation of ideal Ohm's law along the flux tubes. However, where and how fast which dust species evaporate at what distance from the stellar object in the considered non-equilibrium situation is a highly involved matter. In terms of time scales the discussed heating process is slowest in the dusty regime (see below).

## 2. Energy conversion caused by magnetic reconnection: heating versus cooling

### *2.1. First step: the dusty plasma regime*

The quite complicated disk-stellar object interaction in classical TTS results in a twist, i.e. injection of magnetic helicity in closed magnetic loops (cf. Fig. 1). The free energy stored in the associated current sheet can be converted to high-energy particle acceleration (cf. Birk 1998) and plasma heating during explosive events, if some violation of ideal Ohm's law allows for a change of magnetic field topology. Whereas in the initially considered dusty regime the electron-ion momentum transfer should be negligible, collisions with dust and neutral particles, in particular, but not exclusively at the disk boundary of closed flux tubes can easily result in an effective finite electrical conductivity. The evaluation of the appropriate Landau integrals (cf. Benkadda et al. 1996) shows that for the disk regime the ion-dust and dust-neutral collisions are dominant. A generic reconnection process that can be studied in a quantitative way is the resistive tearing instability. In our context this instability must be analyzed for a partially ionized dusty plasma system (Birk et al. 1996; Birk 1998). In some sense when considering the time scales involved in the reconnection process this is the least favorable case, since the macroscopic time scale of such a dusty plasmas is governed by the dust particle inertia which is much larger than the ion inertia relevant for a pure magnetohydrodynamic (MHD) approach. If we can show that even when starting from such a regime the dissipative heating during the reconnection event is fast enough to eventually result in X-ray emission one may feel quite comfortable with the suggested model. However, after the plasma is heated up to temperatures $T \sim 2000\,\mathrm{K}$ the dust component will be evaporated/sublimated and the reconnection process continues in a dust-free regime where the localized resistivity is caused by microturbulence excited in course of the reconnection dynamics (see next subsection).

The efficiency of the heating in reconnection regions is measured by the net effect of Ohmic dissipation on the one side and cooling on the other side. The cooling rate $L$ of a plasma or gas is related to the universal cooling function $\mathcal{L}$ by the expression $L = n_\mathrm{e}^2 \mathcal{L}$ where $n_\mathrm{e}$ denotes the electron density. The cooling function that results from a complicated combination of as different cooling mechanisms as line radiation and bremsstrahlung can be taken from the literature (cf. Dalgarno & McCray 1972).

The irreversible heating $Q$ is given by the Ohmic dissipation $Q = \eta j^2$. In the dusty plasma regime the resistivity $\eta$ is given by

$$\eta = \eta_\mathrm{d} = m_i^2(\nu_\mathrm{id} + \nu_\mathrm{in})/e^2\rho_\mathrm{i} \tag{1}$$

where $e$, $m_\mathrm{i}$ and $\rho_\mathrm{i}$ are the elementary charge, the ion mass and ion mass density and $\nu_\mathrm{id}$ and $\nu_\mathrm{in}$ are the effective ion-dust and ion-neutral collision frequencies, respectively. The electric current density $j$ is a measure of the free energy available, since it is associated with magnetic shear and the length scale of the magnetic field inhomogeneity by Ampères law. For efficient heating $t_\mathrm{cool}/t_\mathrm{heat} = (nk_\mathrm{B}T/L)/(nk_\mathrm{B}T/Q) \gg 1$ should hold ($k_\mathrm{B}$,$n$ and $T$ are the Boltzmann constant and the particle density and temperature of the radiating gas). If we assume for simplicity and analytical handling that the tearing mode is the relevant reconnection process that causes the plasma heating in TTS magnetospheres (cf. Birk 1998) we have $t_\mathrm{X} \sim t_\mathrm{heat} \sim t_\mathrm{tear}$ where $t_\mathrm{tear}$ is the (linear) growth time of the relevant unstable tearing mode. Whereas the observed time scales for X-ray flares are associated with the temporal evolution of their dynamical cause, i.e. the tearing mode, the duration of the flares is not given by the cooling time, since we are not dealing with a static radiating system. Rather, the heated relatively dense plasma will expand and since the bremsstrahlung emissivity scales as the square of the density of the radiating particles the flare luminosity drops much faster below the background X-ray luminosity than one would expect from adiabatic cooling only.

Numerical studies have shown that the dust tearing mode indeed works comparable to the classical MHD one (Birk et al. 1996; Schröer et al. 1998).

The dispersion relation of the tearing instability in partially ionized dusty plasmas reads in a normalized form (Birk 1998):

$$\frac{q^{\frac{1}{2}} k^{\frac{1}{2}} \rho_\mathrm{d}^{\mathrm{eq}\,\frac{1}{4}} \pi}{\eta_\mathrm{d}^{\frac{1}{2}}} \Lambda^{\frac{1}{2}} = (1-\Lambda^2)(1-k^2) \frac{\Gamma\left(\frac{\Lambda+1}{4}\right)}{\Gamma\left(\frac{\Lambda+3}{4}\right)} \tag{2}$$

with

$$\Lambda = \frac{q^{\frac{3}{2}}}{k\eta_{\rm d}^{\frac{1}{2}}}\left(1+\frac{\nu_{\rm dn}}{q+\nu_{\rm nd}}\right)^{\frac{1}{2}} \tag{3}$$

where $\rho_{\rm d}^{\rm eq}$, $q$ and $k$ are the equilibrium dust mass density, the complex growth rate and the wave number of the unstable mode. From the solution of the dispersion relation (Eq. (2)) the linear growth time $t_{\rm tear}^{\rm d}$ (the upper index $d$ indicates the dust tearing time scale) can be found as the product of the inverse of the real part of the normalized growth rate $q$ and the dust Alfvénic transit time $\tau_{\rm A}^{\rm d} = l(4\pi\rho_{\rm d}^{\rm eq})^{\frac{1}{2}}/B^{\rm eq}$ as

$$t_{\rm tear}^{\rm d} = \frac{\tau_{\rm A}^{\rm d}}{q} = \frac{l(4\pi\rho_{\rm d}^{\rm eq})^{\frac{1}{2}}}{qB^{\rm eq}} \tag{4}$$

where $l$ and $B^{\rm eq}$ are the half-thickness of the current sheet of the considered magnetic flux tube and the equilibrium magnetic field strength. The effective collision frequencies of the neutrals, single charged ions and dust particles that are needed for the evaluation of the resistivity $\eta_{\rm d}$ and the growth rate $q$ are given as functions of the particle densities (cf. Benkadda et al. 1996; Huba 1994; note also that $n_\alpha\nu_{\alpha\beta} = n_\beta\nu_{\beta\alpha}$)

$$\nu_{\rm nd} = \frac{4}{3}\frac{(2\pi)^{\frac{1}{2}}z_{\rm d}^2 n_{\rm d}e^2}{m_{\rm n}^2 v_{\rm n}^3} ln\left(\frac{\lambda_{\rm De}}{r_{\rm d}}\right) \tag{5}$$

$$\nu_{\rm id} = \frac{4}{3}\frac{(2\pi)^{\frac{1}{2}}z_{\rm d}^2 n_{\rm d}e^2}{m_{\rm i}^2 v_{\rm i}^3} ln\left(\frac{\lambda_{\rm De}}{r_{\rm d}}\right) \tag{6}$$

$$\nu_{\rm in} = 5\cdot 10^{-15} n_{\rm n} v_{\rm i} \tag{7}$$

where $z_{\rm d}$, $r_{\rm d}$, $m_{\rm i,n}$, $v_{\rm i,n} = (kT_{\rm i,n}/m_{\rm i,n})^{\frac{1}{2}}$ and $\lambda_{\rm De} = (3k_{\rm B}T_{\rm e}/\pi n_{\rm e}e^2)^{\frac{1}{2}}$ are the dust charge number, the dust grain radius, the ion/neutral mass, the ion/neutral thermal velocity and the electron Debye length.

In order to compare the cooling and the heating rate during the heating process that eventually results in the observed X-ray emission one needs to know the temporal evolution of the particle densities $n_\alpha$ for the entire temperature range under consideration. The evaporation/sublimation of the dust with growing temperature can reasonably be modelled by

$$n_{\rm d}(T_d) = n_{\rm d0}\frac{\Theta(T_{\rm d}^{\rm vap} - T_{\rm d})}{1 + aexp(b(T_{\rm d} - T_{\rm d}^{\rm vap0}))} \tag{8}$$

where $T_{\rm d}^{\rm vap} \approx 2000\,{\rm K}$ and $T_{\rm d}^{\rm vap0} \approx 1700\,{\rm K}$ are the temperatures at which the dust is evaporated/sublimated totally and starts evaporating/sublimating, respectively, and $\Theta$ denotes the step function. The index 0 indicates the initial value. The model parameters $a$ and $b$ that determine the details of the dust density profile are a priori unknown, but we are not interested in the details of the evaporation/sublimation process. Here, we choose somewhat arbitrarily $a = 0.1$ and $b = 0.04$. The findings discussed in the next subsection are, however, not influenced significantly by the particular choice of $a$ and $b$. For the neutral gas density, as a first approximation, we make use of the Saha equation

$$n_{\rm n}(T_{\rm n}) = (n_{\rm n0} + n_{\rm i0}) \times \left(1 + \frac{(2\pi m_{\rm e}k_{\rm B}T_{\rm e})^{\frac{3}{4}}}{n_{\rm n0}^{\frac{1}{2}}h^{\frac{3}{2}}} exp(-\frac{13.6eV}{2k_{\rm B}T_{\rm n}})\right)^{-1} \tag{9}$$

where $h$ denotes the Planck constant. For the ion and electron densities we find accordingly

$$n_{\rm i} = n_{\rm i0} + n_{\rm n0} - n_{\rm n}(T_{\rm n}) \tag{10}$$

and

$$n_{\rm e} = n_{\rm e0} + n_{\rm n0} - n_{\rm n}(T_{\rm n}) + z_{\rm d}(n_{\rm d0} - n_{\rm d}(T_{\rm d})). \tag{11}$$

### *2.2. Second step: the dust-free regime*

Once the tearing instability is excited in the dusty plasma regime the considered current sheet becomes microturbulent. This means that besides particle collisions the localized violation of ideal Ohm's law, which is a necessary condition for the reconnection process, can be provided by anomalous resistivity. In this case the electrical resistivity is caused by particle momentum transfer via turbulent electromagnetic fields (e.g. Huba 1985; Benz 1993). After the total evaporation/sublimation of the dust component the anomalous resistivity becomes dominant. In general, it can be written

$$\eta_{\rm an} = f\frac{m_{\rm e}\omega_{\rm e}}{n_{\rm e}e^2} \tag{12}$$

where $\omega_{\rm e} = (4\pi n_{\rm e}e^2/m_{\rm e})^{\frac{1}{2}}$ is the electron plasma frequency. The factor $f \leq 1$ measures the level of turbulent dissipation depending on the kind of microturbulence excited. In our model from a variety of possibly excited microinstabilities we choose the lower-hybrid drift instability (Krall & Liewer 1971; Huba 1985). This kind of instability can be excited very easily and results in a rather low dissipation as compared to fully developed two-stream instabilities. The latter ones cannot be ruled out but the restriction to lower-hybrid microturbulence gives a lower limit for the dissipation and therefore the heating rate achievable (cf. again Huba 1985). The resulting resistivity can be estimated as

$$\eta_{\rm an} = \frac{m_{\rm e}(\omega_{\rm ce}\omega_{\rm ci})^{\frac{1}{2}}}{n_{\rm e}e^2} \tag{13}$$

with the gyrofrequencies $\omega_{\rm ce,ci} = eB/m_{\rm e,i}c$ which results in $f = v_{\rm A}n_{\rm i}^{\frac{1}{2}}/cn_{\rm e}^{\frac{1}{2}}$ where $v_{\rm A} = B^{\rm eq}/(4\pi\rho^{\rm eq})^{\frac{1}{2}}$ is the Alfvén velocity in the dust-free regime. The growth time of the classical resistive tearing mode (Furth et al. 1963) is given by the geometric mean of the Alfvénic transit time and the resistive diffusion time

$$t_{\rm tear} = \left(\frac{4\pi l^3}{c^2\eta_{\rm an}v_{\rm A}}\right)^{\frac{1}{2}}. \tag{14}$$

Birk & Otto (1991) showed that the tearing instability evolves faster, if one considers a non-constant resistivity, e.g. $\eta(n,T)$.

However, in the following, we make use of the classical estimation Eq. (14) which reads for our choice of the microturbulent resistivity

$$t_{\rm tear} = \frac{(4\pi)^{\frac{3}{4}}(em_{\rm i})^{\frac{1}{2}}}{c^{\frac{1}{2}}m_{\rm e}^{\frac{1}{4}}} \frac{l^{\frac{3}{2}}n_{\rm i}^{\frac{1}{4}}n_{\rm e}^{\frac{1}{2}}}{B^{\rm eq}} \tag{15}$$

and is a rather conservative estimate of the time scale of reconnection and dissipative heating.

### *2.3. Model results*

The crucial parameter for the heating rate is the resistivity. We assume that the different plasma components are in ideal thermal contact and model the resistivity over the entire considered temperature range in terms of the effective temperature $T$

$$\eta(T) = \alpha_{\rm d}\eta_{\rm d}(T) + \alpha_{\rm an}\eta_{\rm an}(T) \tag{16}$$

with

$$\alpha_{\rm d} = \Theta(T_{\rm d}^{\rm vap0} - T) + \Theta(T - T_{\rm d}^{\rm vap0})\Theta(T_{\rm d}^{\rm vap} - T) \times \left(1 - \frac{T - T_{\rm d}^{\rm vap0}}{T_{\rm d}^{\rm vap} - T_{\rm d}^{\rm vap0}}\right) \tag{17}$$

and

$$\alpha_{\rm an} = \Theta(T - T_{\rm d}^{\rm vap0})\Theta(T_{\rm d}^{\rm vap} - T)\frac{T - T_{\rm d}^{\rm vap0}}{T_{\rm d}^{\rm vap} - T_{\rm d}^{\rm vap0}} + \Theta(T - T_{\rm d}^{\rm vap}). \tag{18}$$

This choice of form functions allows for a reasonable description of the functional dependence of the resistivity on temperature. Fortunately, again, we do not have to dwell on the details of the complex process of dust evaporation/sublimation.

Eq. (16) is the final equation we do need to model the heating and cooling in the temporally varying plasma regimes. In the following we present model results for three different sets of parameters without changing the mass, the radius and the charge of the dust particles chosen as $m_{\rm d} = 10^3 m_{\rm i}$, $r_{\rm d} = 10^{-8}$ cm and $z_{\rm d} = 100$. The model results are not very sensitive to these quantities. The specifications for the magnetic field, namely the length scale of the inhomogeneity and the strength of it, are more crucial. We choose for the length scale, i.e. the half thickness of the current sheets $l = 10^{10}$ cm which is comparable to the spatial extent of the whole emitting flux tube (e.g. Montmerle 1991 and references therein). The real thickness of the current sheets involved in the reconnection process is expected to be orders of magnitude thinner. Thus, our choice gives a lower limit for the heating rate and an upper limit for the time scale of the reconnection driven plasma heating. For the magnetic field strength we choose $B^{\rm eq} = 150$G consistent with observations and analytical models that indicate kG fields on the surface of the stellar object (cf. Montmerle 1991, André 1996). Note that the tearing growth time scales as $t_{\rm tear}^{\rm d} \sim l/B^{\rm eq}$ and $t_{\rm tear} \sim l^{3/2}/B^{\rm eq}$ and the heating rates as $Q^{\rm d} = \eta^{\rm d} j^2 \sim {B^{\rm eq}}^2/l^2$ and $Q = \eta_{\rm an} j^2 \sim {B^{\rm eq}}^3/l^2$, respectively. Figs. 2–4 show model results of the evolution of the resistivity (eta) (middle plots) and the ratio of heating to cooling (Q/L) (lower plots) with temperature for different ini-

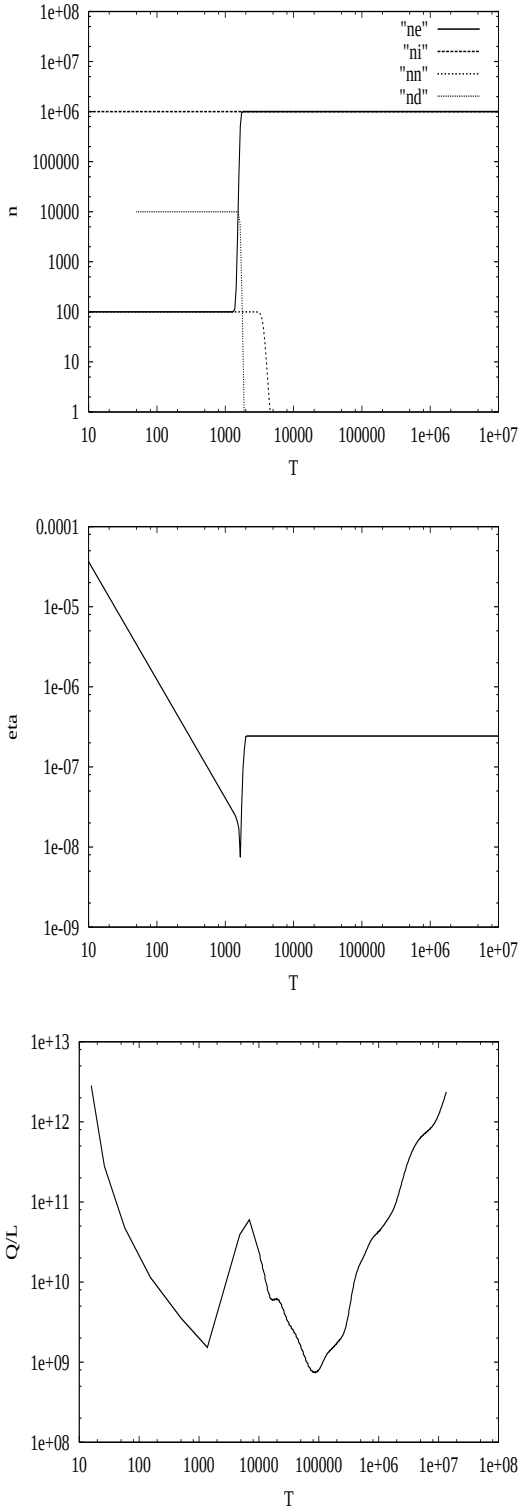


**Fig. 2.** Model results for the particle number densities (upper plot), the resistivity (middle plot), and $Q/L$, i.e. heating vs. cooling, (lower plot) as functions of the effective temperature $T$. The initial particle densities are chosen as: $n_{\rm e0} = n_{\rm n0} = 10^2{\rm cm}^{-3}$, $n_{\rm i0} = 10^6{\rm cm}^{-3}$ and $n_{\rm d0} = 10^4{\rm cm}^{-3}$.

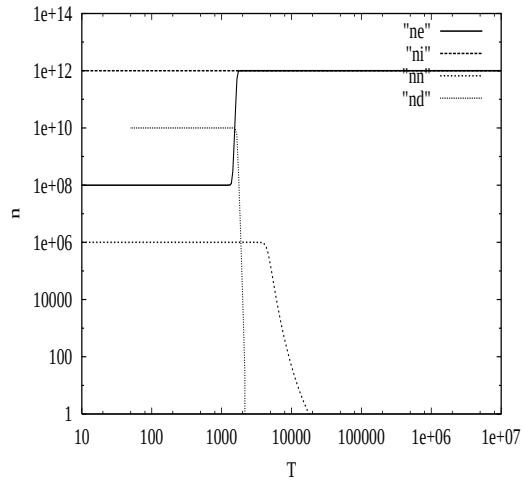


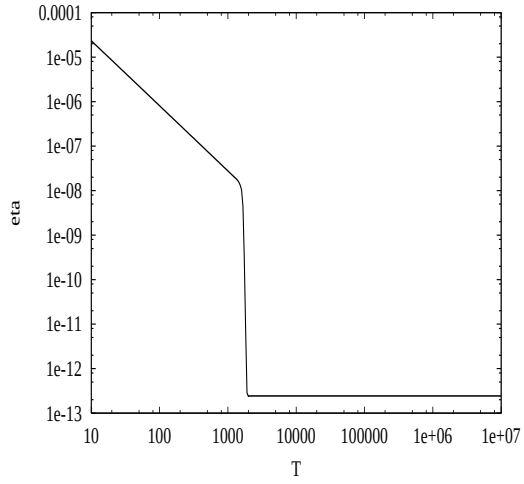


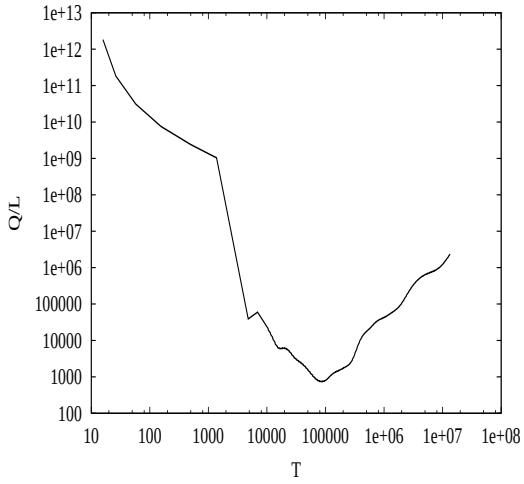


**Fig. 3.** Same as in Fig. 2 for different initial particle number densities. The initial particle densities are chosen as: $n_{\rm e0} = 10^8 {\rm cm}^{-3}$, $n_{\rm i0} = 10^{12} {\rm cm}^{-3}$, $n_{\rm d0} = 10^{10} {\rm cm}^{-3}$ and $n_{\rm n0} = 10^6 {\rm cm}^{-3}$.

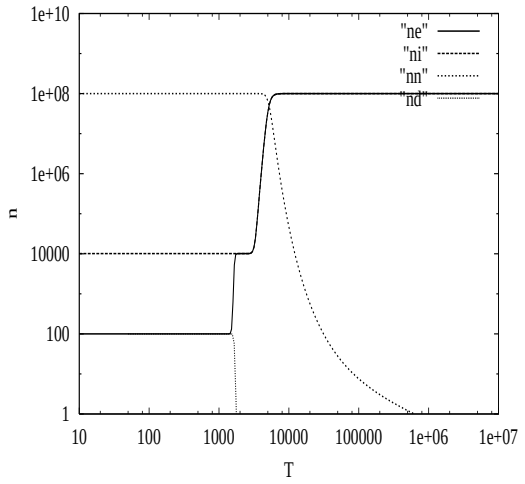


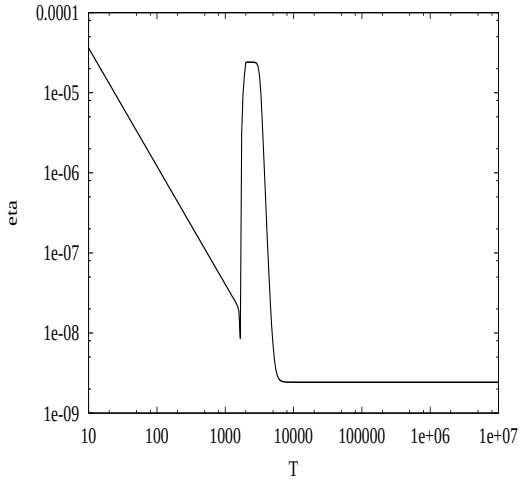


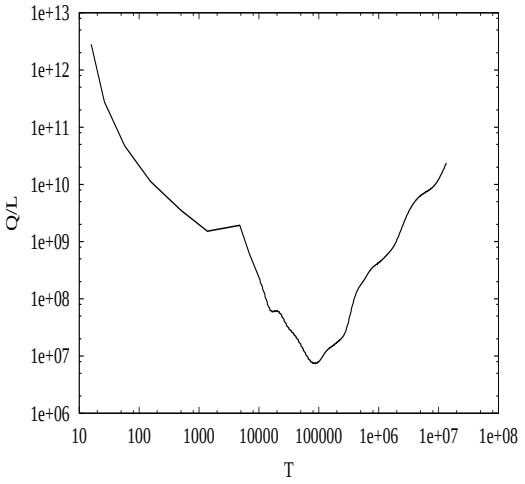


**Fig. 4.** Same as in Fig. 2 for different initial particle number densities. The initial particle densities are chosen as: $n_{\rm e0} = n_{\rm d0} = 10^2 {\rm cm}^{-3}$, $n_{\rm i0} = 10^4 {\rm cm}^{-3}$ and $n_{\rm n0} = 10^8 {\rm cm}^{-3}$.

tial particle densities (upper plots). The results take into account dust evaporation/sublimation as well as ionization. The particle densities are varied over a wide range of orders of magnitude. The drop in $Q/L$ at about $10^4$ K is caused by the jump in the cooling function where recombination is dominant. For realistic particle densities the dissipative heating mechanism in the localized reconnection regions is more efficient than cooling by many orders of magnitude. Even for very high electron densities

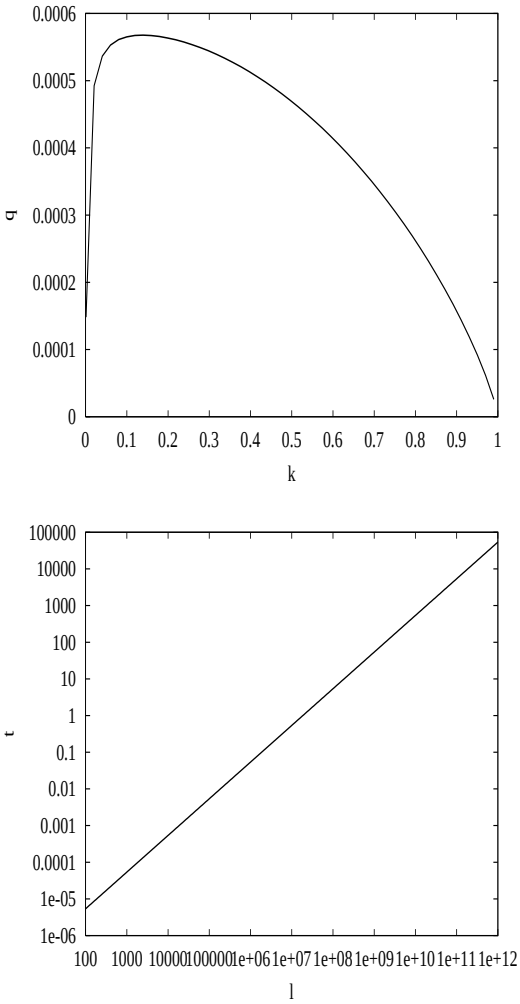


**Fig. 5.** The dispersion relation of the dust tearing mode (upper plot) and the functional dependence of the associated linear growth time (cf. Eq. (4)) of the most unstable mode on the scale length $l$ (lower plot). The growth rate $q$ and the wave number $k$ are given in normalized units, i.e. $1/q = t^{\rm d}_{\rm tear}/\tau^{\rm d}_{\rm A}$ and $k = 2\pi l/\lambda$ ($\lambda$ denotes the wavelength of the mode) whereas the time scale $t$ and the length scale $l$ are given in Gaussian units. The number densities are chosen as in Fig. 2.

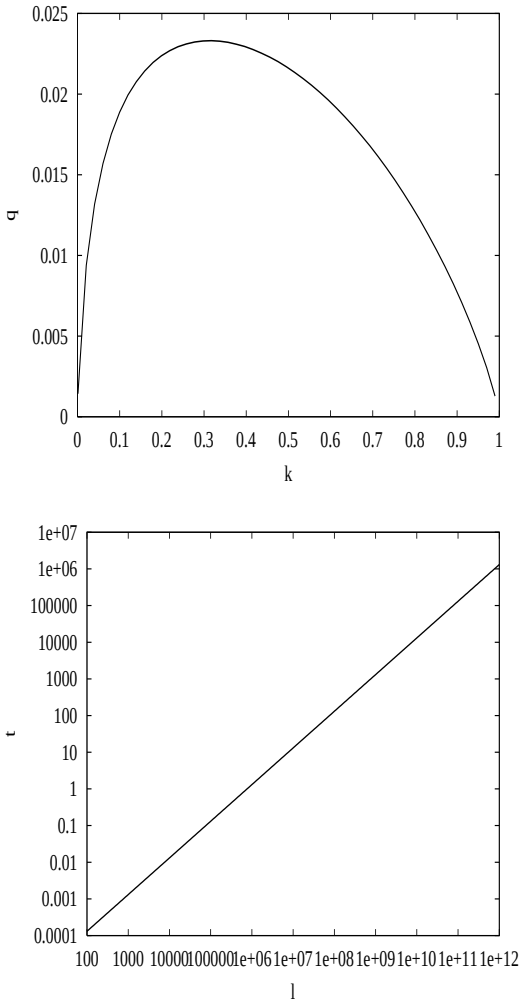


**Fig. 6.** Same as in Fig. 5. The number densities are chosen as in Fig. 3.

(cf. Fig. 3) efficient heating is guaranteed. In this case also the crucial cooling barrier at $T = 10^4$ K can be overcome by the dissipative heating due to magnetic energy conversion.

Figs. 5–7 show the dust tearing dispersion relation in normalized units and the respective time scales (this time as functions of the not fixed length scale $l$) for reconnection and heating in the dusty phase for the parameters of Figs. 2–4. After the evaporation/sublimation of the dust the tearing mode evolves on the time scales governed by the anomalous dissipation. Fig. 8 shows the time scale for the quasineutral case ($n = n_{\rm e} = n_{\rm i}$) and $B^{\rm eq} = 150$G plotted against the particle density $n$ (cf. Fig. 8a, $l = 10^{10}$ cm) and the characteristic length scale $l$ (Fig. 8b, $n = 10^5 {\rm cm}^{-3}$) in double logarithmic representation. In the context of the proposed reconnection scenario the observed variety of flare time scales of some $10$ seconds to some hours can be regarded as a natural consequence of different sizes of magnetic flux tube in which the reconnection events occur.

## 3. Discussion

We have shown that dissipative heating in reconnection regions in T-Tauri magnetospheres is fast and efficient enough to be responsible for X-ray flares. In this contribution we analyzed the heating process starting from the cold partially-ionized dusty plasma regime where collisional resistivity is dominant and ending with a dust-free totally ionized plasma where anomalous resistivity causes the violation of ideal Ohm's law. The highly variable time scales of flares can be explained in terms of varying plasma parameters and degree of filamentary structure, i.e. thickness of the considered current sheets that are unstable against the tearing modes.

It is worth mentioning that for the cold dusty plasma regime and up to temperatures of some $10^5$ K the general cooling function $\mathcal{L}$ is growing with temperature. Therefore, no coupled radiative tearing mode (Tachi et al. 1983; Steinolfson & van Hoven 1984) that results in higher growth rates as compared to the radiation free mode is to be expected. For higher temperatures in

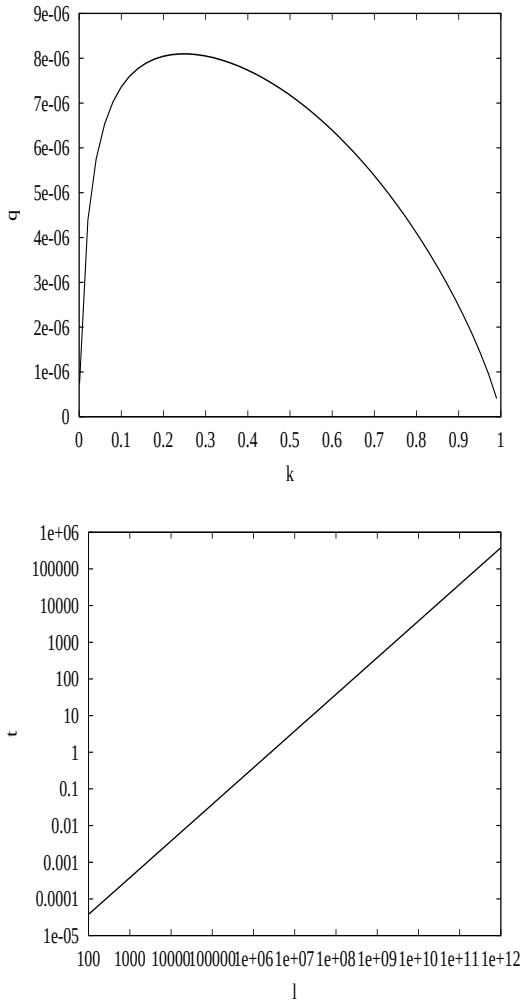


**Fig. 7.** Same as in Fig. 6. The number densities are chosen as in Fig. 4.

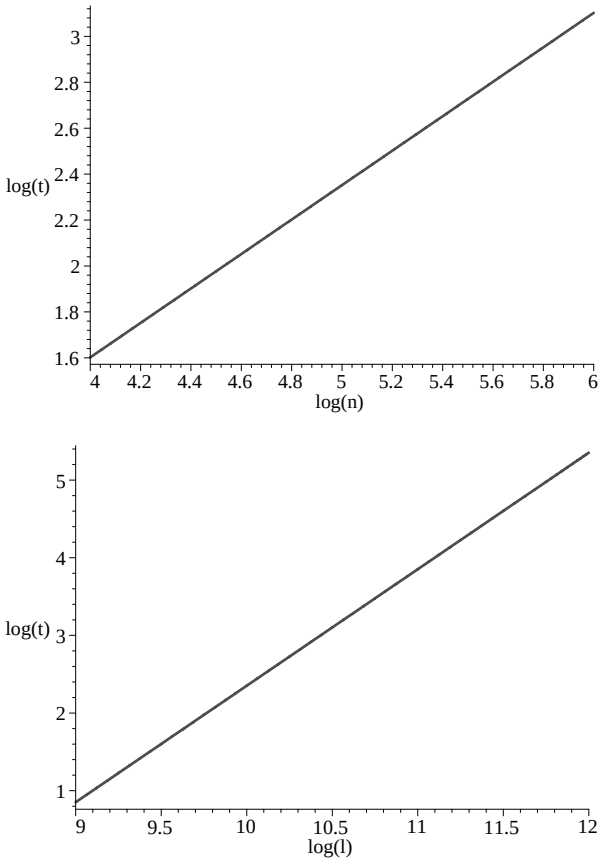


**Fig. 8.** The linear time scale of the resistive dust-free tearing mode as a function of the particle density $n$ and the length scale $l$ in double-logarithmic representation. Here, units are Gaussian. The magnetic equilibrium magnetic field is chosen as $B^{\rm eq} = 150$G and in Fig. 8a and Fig 8b $l = 10^{10} cm$ and $n = 10^5 {\rm cm}^{-3}$, respectively.

the fully ionized regime the coupling of the radiative and the resistive modes may result in shorter linear time scales as the ones used in our analysis.

In the proposed reconnection model the energy for the heating process is supplied by magnetic shear. For the parameters chosen in our analysis in the radiating volume $V$ the magnetic field energy of $W_{\rm B} = (150{\rm G})^2/8\pi V$ can, in principle, be converted to heat (and charged particle acceleration). In order to account for the observed luminosities up to $L_{\rm X} \approx 10^{34} {\rm ergs}^{-1}$ a significant fraction of the sheared field component must be dissipated in a volume $V$ with linear sizes of about $l \approx 10^{10}$ cm. In the scenario we have in mind multiple reconnection events take place in the flux tube topology that constitutes T-Tauri magnetospheres. In the emitting volume, filamentary relatively thin current sheets are sites of reconnection events rather than one thick current sheet (for the aspect of filamentation in this context see, e.g., discussion by Horiuchi & Sato 1997; Wiechen et al. 1998). It should be noted that the shear component of the magnetic field dissipated into heat is continuously built up again due to the ongoing injection of magnetic helicity.

Whereas the present analytical work is restricted to linear theory numerical simulation studies of the non-linear evolution of tearing modes in T-Tauri magnetospheres would give important additional insight in the physics of X-ray phenomena in young stellar objects that are observed not only in T-Tauri magnetospheres but also in protostellar class I objects (cf. Koyama et al. 1996; Grosso et al. 1997).

*Acknowledgements.* We would like to thank the referee for his helpful comments on the original version of the manuscript. This work was supported by the Deutsche Forschungsgemeinschaft through the Schwerpunkt "Physik der Sternentstehung" (LE-1039/3-1).

## References

André P. 1996, In: Taylor A.R., Paredes J.M., (eds.) Radio Emission from the Stars and the Sun, ASP Conf. Ser. 93, p. 273

Benkadda S., Gabbai P., Tsytovich V.N., Verga A. 1996, Phys. Rev. E 53, 2717

Benz A.O., 1993, Plasma Astrophysics. Dordrecht: Kluwer

Birk G.T., Otto A., 1991, Phys. Fluids B 3, 1746

Birk G.T., Kopp A., Shukla P.K., 1996, Phys. Plasmas 3, 3564

Birk G.T., 1998, A&A 330, 1070

Carkner L., Feigelson E.D., Koyama K., Montmerle T., Reid I.N., 1996, ApJ 464, 286

Dalgarno A., McCray R.A., 1972, ARA&A 10, 375
Feigelson E.D., DeCampli W.M., 1981, ApJ 243, L89
Feigelson E.D., Montmerle T., 1999, ARA&A 37, 363
Furth H.P., Killeen J., Rosenbluth M.N., 1963, Phys. Fluids 6, 459
Grosso N., Montmerle T., Feigelson E.D., et al., 1997, Nat 387, 56
Gullbring E., Barwig H., Schmitt J.J., 1997, A&A 324, 155
Hayashi M.R., Shibata K., Matsumoto R. 1996, ApJ 468, L37
Hirose S., Uchida Y., Shibata K., Matsumoto R., 1997, PASJ 49, 193
Huba J.D., 1985, In: Kundu M.R., Holman G.D. (eds.), Unstable Current Systems and Plasma Instabilities in Astrophysics, IAU 107. Dordrecht: Reidel, p. 233
Huba J.D., 1994, NRL Plasma Formulary, Washington DC, p. 39
Horiuchi R., Sato T., 1997, Phys. Plasmas 4, 277
Koyama K., Hamaguchi K, Ueno S., Kobayashi N., Feigelson E.D., 1996, PASJ 48, L87
Krall N.A., Liewer P.C., 1971, Phys. Rev. A 4, 2094
Kuijpers J., Kuperus M., 1995, A&A 286, 491
Lesch H., Birk G.T., 1997, A&A 324, 61
Li J., 1996, ApJ 456, 696
Miller K.A., Stone J.M., 1997, ApJ 489, 890
Montmerle T., 1991, In: Lada C.J., Kylatis N.D. (eds.), The Physics of Star Formation and Early Stellar Evolution, Dordrecht: Kluwer, p. 675
Preibisch T., Zinnecker H., Schmitt J.H., 1993, A&A 279, L33
Schopper R., Lesch H., Birk G.T., 1998, A&A 335, 26
Schröer A., Birk, G.T., Kopp, A., 1998, Comp. Phys. Comm. 112, 7
Steinolfson R.S., van Hoven G., 1984, ApJ 276, 391
Tachi T., Steinolfson R.S., van Hoven G., 1983, Phys. Fluids 26, 2976
Tsuboi Y., Koyama K., Murakami H., et al., 1998, ApJ 503, 894
Wiechen H., Birk G.T., Lesch H., 1998, Phys. Plasmas 5, 3732